

Stochastic resonance with applied and induced fields: the case of voltage-gated ion channels

M. Shaked ¹, Z. Schuss ²

Abstract

We consider a charged Brownian particle in an asymmetric bistable electrostatic potential biased by an externally applied or induced time periodic electric field. While the amplitude of the applied field is independent of frequency, that of the one induced by a magnetic field is. Borrowing from protein channel terminology, we define the open probability as the relative time the Brownian particle spends on a prescribed side of the potential barrier. We show that while there is no peak in the open probability as the frequency of the *applied* field and the bias (depolarization) of the potential are varied, there is a narrow range of low frequencies of the *induced* field and a narrow range of the low bias of the potential where the open probability peaks. This manifestation of stochastic resonance is consistent with experimental results on the voltage gated I_{Ks} and KCNQ1 potassium channels of biological membranes and on cardiac myocytes.

1 Introduction

Our recent experimental findings show unusual non-thermal biological effects of a periodic electromagnetic field (EMF) of frequency 16 Hz and amplitude 16 nT (nano Tesla) on the potassium current in human I_{Ks} and KCNQ1 channels [1]. More specifically, we expressed the I_{Ks} channel in *Xenopus* oocytes and varied the membrane depolarization between -100 mV and +100 mV and measured the membrane potassium current. The current with applied EMF peaked above that without applied EMF at membrane depolarizations between 0 mV and 8 mV to a maximum of about 9% (see Figures 1 and 2). A similar measurement of the potassium current in the KCNQ1 channel protein, expressed in an oocyte, gave a maximal increase of 16% at the same applied EMF and at membrane depolarizations between -10 mV and -3 mV (see Figure 3). Similar experiments with L-type calcium channels showed no response to the electromagnetic field at any frequency between 0.05 and 50 Hz.

In a related experiment [2], we applied electromagnetic fields at frequencies 15 Hz, 15.5 Hz, 16 Hz, 16.5 Hz and amplitudes of the magnetic field from below 16 pT and up to 160 nT, to neonatal rat cardiac myocytes in cell culture. In the range 16 pT – 16 nT, we observed that both stimulated and spontaneous activity of the myocytes changed at frequency 16 Hz: the height and duration of cytosolic calcium transients began decreasing significantly about 2 minutes after the magnetic field was applied and kept decreasing for about 30 minutes until it stabilized at about 30% of its initial value and its width decreased to approximately 50%. About 10 minutes following cessation of the magnetic field the myocyte (spontaneous)

¹Department of Systems, School of Electrical Engineering, The Iby and Aladar Fleischman Faculty of Engineering, Tel-Aviv University, Ramat-Aviv Tel-Aviv 69978, Israel.

²Department of Mathematics, Tel-Aviv University, Tel-Aviv 69978, Israel.

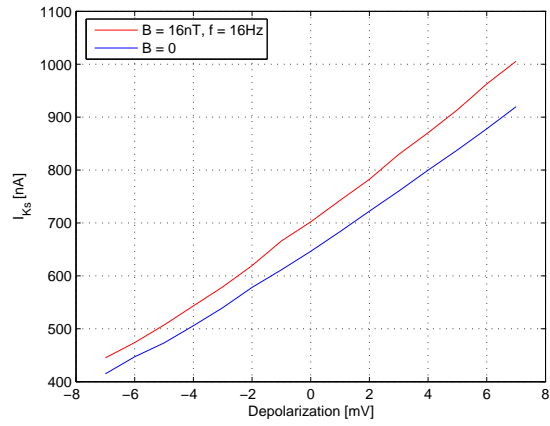


Figure 1: I_{Ks} current in *Xenopus* oocytes with applied magnetic field of 16 Hz and 16 nT (red) and without (blue)

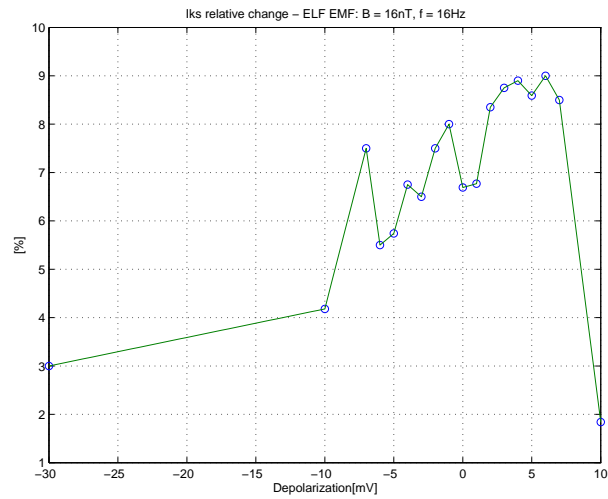


Figure 2: The quotient of I_{Ks} expressed in *Xenopus* oocytes with applied magnetic field of 16 Hz and 16 nT and without (red to blue in Figure 1)

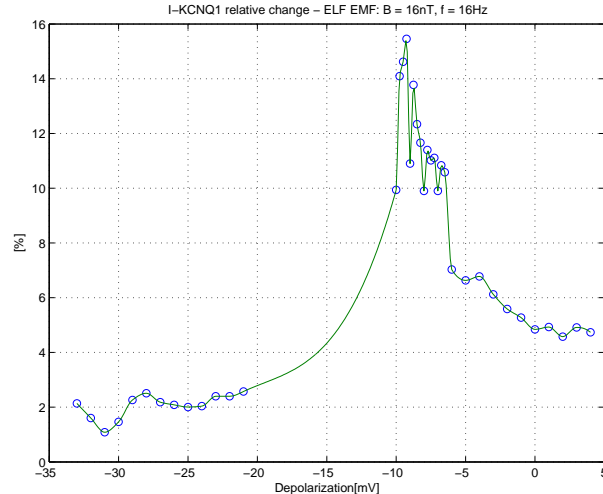


Figure 3: The quotient of KCNQ1 expressed in *Xenopus* oocytes with applied magnetic field of 16 Hz and 16 nT and without

activity recovered with increased amplitude, duration, and rate of contraction. Outside this range of frequencies and magnetic fields no change in the transients was observed (see Figure 4). When the stereospecific inhibitor of KCNQ1 and I_{Ks} channels chromanol 293B was applied, the phenomenon disappeared, which indicates that the I_{Ks} and KCNQ1 potassium channels in the cardiac myocyte are the targets of the electromagnetic field, in agreement with the former experiment. The effect of changing the outward potassium current in a cardiac myocyte is to change both the height and duration of calcium transients, action potential, sodium current, as indicated by the Luo-Rudy model [3].

The specific response at 16 Hz may indicate some form of resonance or stochastic resonance of a gating mechanism of open voltage-gated potassium channels (e.g., a secondary structure or mechanism) with time-periodic induced electric field. Since the induced electric field is too low to interact with any component of the I_{Ks} channel, we conjecture that the induced field may interact with locally stable (metastable) configurations of ions inside the selectivity filter [4]. We propose an underlying scenario for this type of interaction based on the collective motion of three ions in the channel, as represented in the molecular dynamics simulation of [4]. The configurations of three potassium ions in the KcsA channel is represented in [4] in reduced reaction coordinates on a three-dimensional free energy landscape. In our simplified model, we represent the collective motion of the three ions in the channel as diffusion of a higher-dimensional Brownian particle in configuration space. An imitation hypothetical energy landscape with a reaction path (indicated in red) is shown in Figures 5 and 6. Projection onto a reaction path reduces this representation to Brownian motion on one-dimensional landscape of potential barriers (see Figure 7). The stable states represent instantaneous crystallization of the ions into a metastable configuration, in which no current flows through the channel, that is, they represent closed states of the channel. There is also a pathway in the multidimensional energy landscape that corresponds to a steady

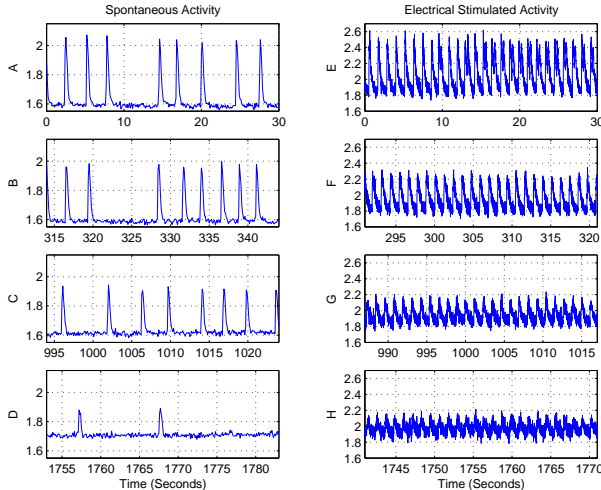


Figure 4: Cardiac cells, 4 days in culture, were exposed to magnetic fields of magnitude 160 pT and frequency 16 Hz for 30 min. Characteristic traces of spontaneous cytosolic calcium activity (A,B,C,D) and of electrically stimulated (1 Hz) cytosolic calcium activity (E,F,G,H). Times are measure in seconds from the moment of application of the magnetic field.

current flowing in the channel, e.g., an unobstructed trough in the energy landscape. Transitions from the latter into the former represent gating events. In our scenario the motion between closed states is simplified to one-dimensional Brownian motion, e.g., in a trough obstructed with barriers, while the interruptions in the current correspond to exits from the unobstructed trough into the obstructed one. Activated transitions over barriers separating two closed states in the obstructed trough (see Figure 8) affect the probability of transition from closed to open states. Stochastic resonance between two closed states may change the transition rates between them, thus affecting the open (or closed) probability of the channel (see Section 4).

We investigate the stochastic resonance (SR) in our mathematical model of a Brownian particle in an *asymmetric* bistable potential with an *induced* electric field. The difference between this problem and that of the extensively studied SR with an *applied* periodic electric field [5], [6] is that according to Faraday’s law (or Maxwell’s equations), the amplitude of the induced field is proportional to the frequency of the applied magnetic field. While the traditional manifestation of SR is a peak in the power spectral density of the trajectory of the resonating particle, we consider its manifestation in the probability to be in one of the two meta-stable states. This measure of SR is ineffective for a symmetric potential, because this probability is 1/2 in the symmetric case and is independent of the applied periodic field. It is effective, however, in asymmetric potentials, for example, when a constant bias field depolarizes the membrane, as is the case in the above mentioned experiments. Note that in the second experiment the depolarization of the myocyte membrane is due to the action potential in the cell. In contrast, asymmetry of the potential can weaken SR with an applied field, as shown in [7], [8].

Our main results concern SR with applied and with induced external periodic forces. In the former case, which we view as a benchmark for our method of analysis, we find that

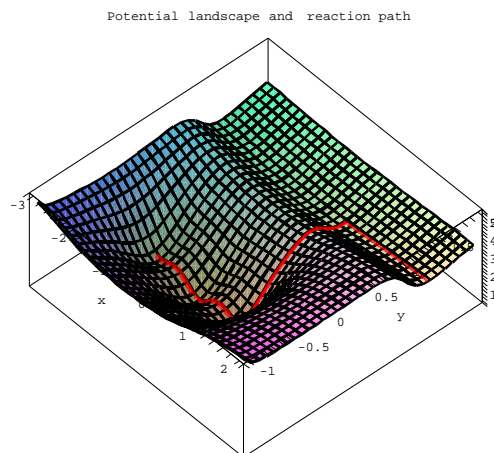


Figure 5: Hypothetical energy landscape of two ions in the selectivity filter. The reaction path is marked red. The straight segment in the trough may represent the open state in the channel

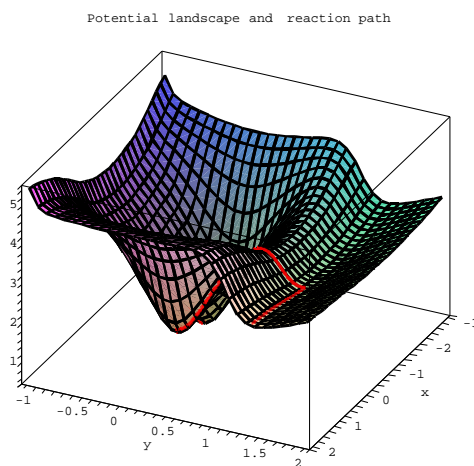


Figure 6: Another view of the hypothetical energy landscape of two ions in the selectivity filter.

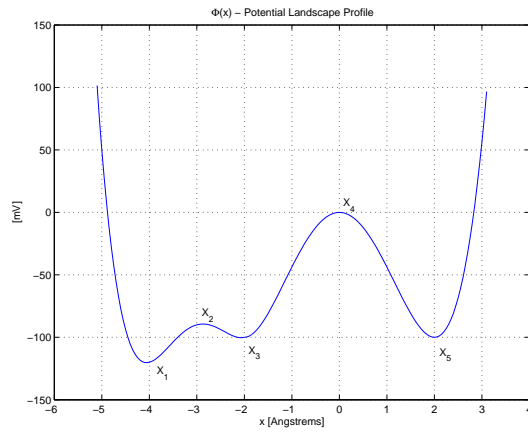


Figure 7: Profile of one-dimensional electrostatic potential landscape biased by a constant electric field

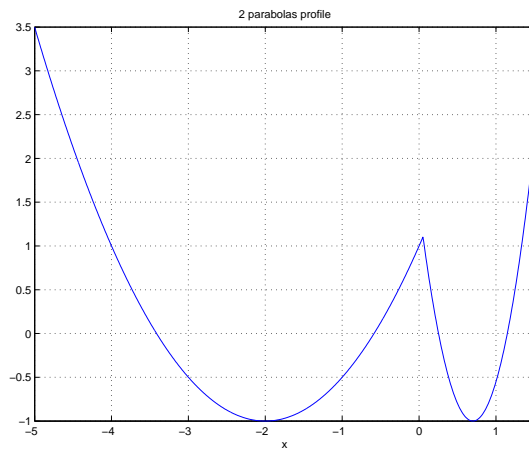


Figure 8: A simplified version (see eq.(3)) of the wells in Figure 7. The wells at x_1 and x_3 and the barrier at x_2 are now at $x_1 = -2$, $x_3 = 0.7$ and $x_2 = 0$. The constant bias in (2) is $c = 0$.

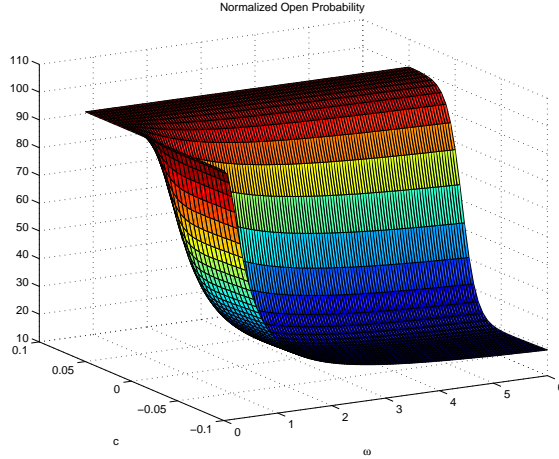


Figure 9: $P_o(\omega, c)/P_o(0, c)$ with induced force A , $A = 0.007, \varepsilon = 0.029, x_L = -2.4, x_R = 1.385$ for $0 < \omega < 6, -0.1 < c < 0.1$. Evidently, there is no SR.

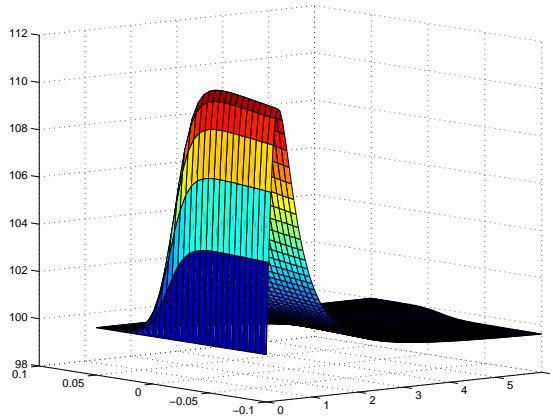


Figure 10: $P_o(\omega, c)/P_o(0, c)$ with induced force $A\omega$, $A = 0.007, \varepsilon = 0.029, x_L = -2.4, x_R = 1.385$

there is no SR as frequency and depolarization are varied, in agreement with known results [5] (see Figure 9). In contrast, the probability to be on one side of the barrier in the case of an induced field peaks at a nearly fixed frequency in a finite window of depolarizations (see Figure 10). We refer to this peak as stochastic resonance, though it may not be the usual SR phenomenon. The folding of the surface in Figure 9 into that in Figure 10 seems to be due to the decrease in the amplitude of the induced field at low frequencies. This observation is consistent with the above mentioned experiments and seems to be new.

To connect the above SR with the cardiac myocyte experiment, we use the Luo-Rudy model [3] of a ventricular cardiac myocyte of a Guinea pig. We express the manifestation of the above SR in the Hodgkin-Huxley equations [9] as a change in the conductance of the I_{Ks} channel in the specific range of depolarizations at the resonant frequency of 16 Hz. We note that the I_{Ks} is one of the delayed rectifier K^+ channels that are present in cardiac myocytes [10], in neuron cells [11], [12], and more, that is, it stays open long enough for its

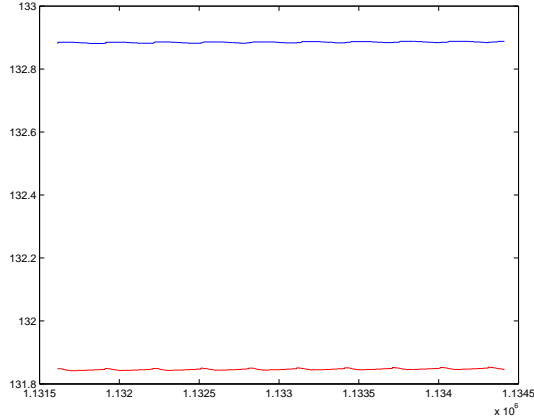


Figure 11: Cytosolic potassium concentration [mM] vs time [msec] without SR (blue) and with SR (red) in the Luo-Rudy model. **SPECIFY UNITS**

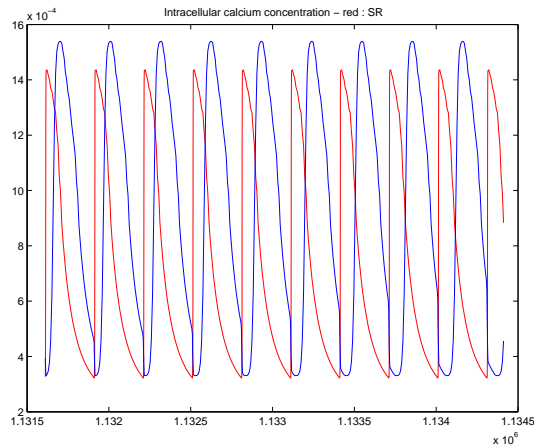


Figure 12: Cytosolic calcium concentration [mM] vs time [msec] without SR (blue) and with SR (red) in the Luo-Rudy model.

(secondary) gating to partially synchronize with the induced field. The SR-increased efflux of potassium (see Figure 11) shortens the action potential, and consequently lowers the peak of the cytosolic calcium concentration (see Figure 12), at the expense of increased sodium concentration (see 13). The shortening of the action potential leads to the shortening of the QT interval (see Figures 14, 15) [10] and was actually observed experimentally [13], [14]. These predictions of the SR modified Luo-Rudy equations are also new. In addition, we obtain from the SR modified Luo-Rudy model an increased conductance during the plateau of the action potential in the cardiac myocyte. This in turn shortens both the action potential and the cytosolic calcium concentration spike durations, lowers their amplitudes, increases cytosolic sodium, and lowers cytosolic potassium concentrations. These theoretical predictions are supported by experimental measurements. Specifically, these effects were communicated in [13], [14], as well as in our own measurements [2].

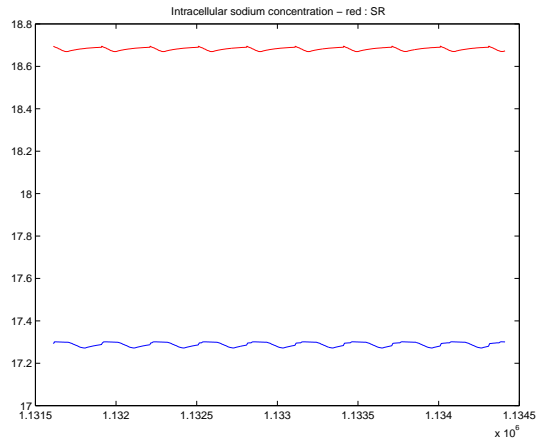


Figure 13: Cytosolic sodium concentration concentration [mM] vs time [msec] without SR (blue) and with SR (red) in the Luo-Rudy model.

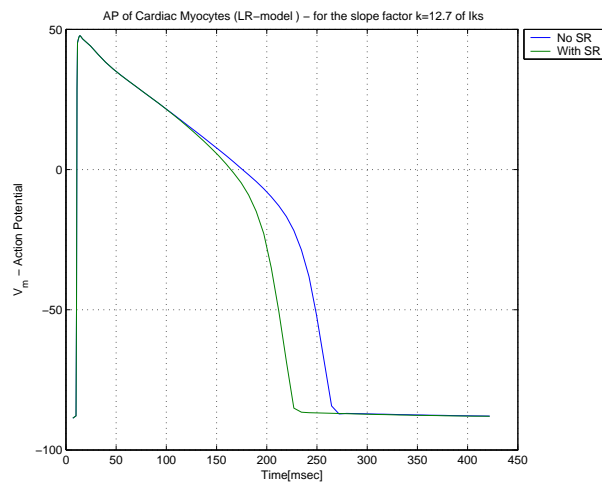


Figure 14: Action potential [mV] vs time [msec] without SR (Blue) and with SR (Green) in the Luo-Rudy model

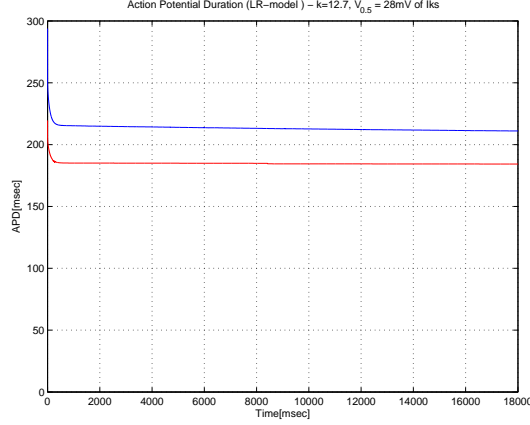


Figure 15: Action potential duration [msec] vs time [msec] without SR (Blue) and with SR (Red) in the Luo-Rudy model.

2 The mathematical model

We consider the dimensionless overdamped dynamics

$$\dot{x} = -\frac{\partial\phi(x, t)}{\partial x} = -\phi_x(x, t) \quad (1)$$

in the bistable time-periodic potential

$$\phi(x, t) = (c - A_{\text{Appl,Ind}}) \sin \omega t x + \phi_0(x), \quad (2)$$

where $A_{\text{Appl,Ind}}$ is the amplitude of the applied (induced) electric field and $\phi_0(x)$ is a fixed parabolic double well potential that consists of the two parabolas

$$\phi_0(x) = \begin{cases} \frac{(x - x_L)^2}{x_L^2} - 1 & \text{for } x < 0 \\ \frac{(x - x_R)^2}{x_R^2} - 1 & \text{for } x > 0, \end{cases} \quad (3)$$

where $x_L < 0 < x_R$. The amplitude of the electric field induced by the time-periodic magnetic field $B \cos \omega t$ ($B = \text{const}$) is $A_{\text{Ind}} = A\omega$, where $A = CB$ and C is the proportionality constant in Faraday's law. The linear term cx represents the membrane depolarization. This model can be considered the limit of the parabolic double well potential that consists of the three parabolas

$$\phi_0(x) = \begin{cases} \frac{(x - x_L)^2}{x_L^2} - 1 + \frac{1}{1 + ax_L^2/2} & \text{for } x < -x_{\delta_L} \\ -\frac{ax^2}{2} & \text{for } -x_{\delta_L} < x < x_{\delta_R} \\ \frac{(x - x_R)^2}{x_R^2} - 1 + \frac{1}{1 + ax_R^2/2} & \text{for } x > x_{\delta_R}, \end{cases} \quad (4)$$

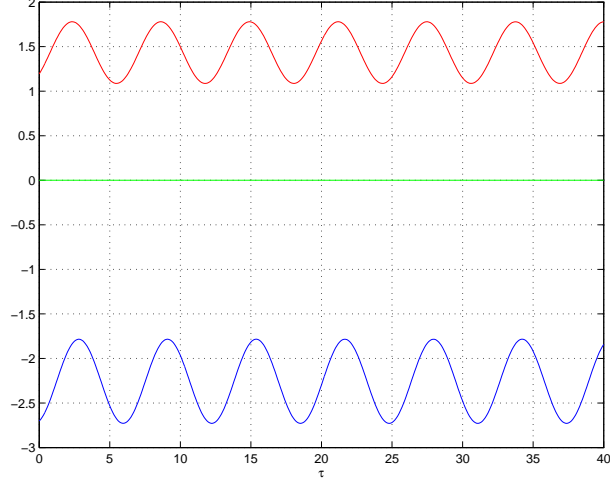


Figure 16: The deterministic trajectories (in dimensionless units) with $\omega = 1$, $A = 0.5$, $c = -0.05$, $x_L = -2.4$, $x_R = 1.385$ are attracted to the periodic $\tilde{x}_L(t)$ (blue lower curve), $\tilde{x}_M(t)$ (green middle curve) and $\tilde{x}_R(t)$ (red upper curve).

where $x_L < -x_{\delta_L} < 0 < x_{\delta_R} < x_R$ and $a > 0$. The three parabolas connect smoothly at $-x_{\delta_L}$ and x_{δ_R} , which implies the relationships $x_{\delta_L} = -\frac{x_L}{1 + ax_L^2/2}$, $x_{\delta_R} = \frac{x_R}{1 + ax_R^2/2}$, $\lim_{a \rightarrow \infty} ax_{\delta_L} = -2/x_L$ and $\lim_{a \rightarrow \infty} ax_{\delta_R} = 2/x_R$. The potential $\phi(x, t)$ (see Figure 8) has two periodic attractors, $\tilde{x}_L(t)$ and $\tilde{x}_R(t)$ (see Figure 16) and the separatrix³ $\tilde{x}_M(t) = 0$. The attractors are the stable periodic solutions of (1), given by

$$\tilde{x}_i(\tau) = \alpha_i - \tilde{A}_i \cos(\tau + \tilde{\varphi}_i), \quad i = L, R \quad (5)$$

$$\tilde{A}_i = \frac{A_{Appl, Ind} x_i^2}{\sqrt{4 + x_i^4 \omega^2}}, \quad \tilde{\varphi}_i = \arctan \frac{2}{x_i^2 \omega}, \quad \alpha_i = \left(x_i - \frac{cx_i^2}{2} \right). \quad (6)$$

When small white noise $\sqrt{2\varepsilon} \dot{w}(t)$ is added to the dynamics (1), it becomes the stochastic equation

$$\dot{x} = -\phi_x(x, t) + \sqrt{2\varepsilon} \dot{w}(t). \quad (7)$$

The trajectories of (7) spend relatively long periods of time near the attractors $\tilde{x}_L(t)$ and $\tilde{x}_R(t)$, crossing $\tilde{x}_M(t)$ at random times. The first passage time from $\tilde{x}_L(t)$ to $\tilde{x}_R(t)$ is defined as

$$\tau_L(t_0) = \inf\{t > 0 : x(t_0) = \tilde{x}_L(t_0), x(t_0 + t) = \tilde{x}_R(t_0 + t)\} \quad (8)$$

and the mean first passage time is defined as

$$\bar{\tau}_L = \frac{1}{T} \int_0^T \mathbb{E} \tau_L(t_0) dt_0, \quad (9)$$

³In the model (4) of three parabolas the separatrix is $\tilde{x}_M(t) = \frac{c}{a} - \left(\frac{A\omega}{a^2 + \omega^2} \right) [\omega \cos \omega t + a \sin \omega t]$.

where \mathbb{E} denotes ensemble averaging over trajectories of (7) and the period is

$$T = \frac{2\pi}{\omega}.$$

The first passage time $\tau_R(t_0)$ and the mean first passage time $\bar{\tau}_R$ are defined in an analogous manner. The fraction of time the random trajectory $x(t)$ spends in the basin of attraction of $\tilde{x}_R(t)$, that is, the fraction of time that $x(t) > \tilde{x}_M(t)$, is the *right probability* $P_R(c, \omega, A_{Appl, Ind}, \varepsilon)$, given by

$$\begin{aligned} P_R(c, \omega, A_{Appl, Ind}, \varepsilon) &= \lim_{n \rightarrow \infty} \frac{1}{nT} \int_0^{nT} \int_{\tilde{x}_M(t)}^{\infty} p(x, t) dx dt \\ &= \lim_{n \rightarrow \infty} \frac{1}{T} \int_0^T \int_{\tilde{x}_M(t+nT)}^{\infty} p(x, t+nT) dx dt \\ &= \frac{1}{T} \int_0^T \int_{\tilde{x}_M(t)}^{\infty} p_{\infty}(x, t) dx dt, \end{aligned} \quad (10)$$

where $p(x, t)$ is the transition probability density function (pdf) of the random process $x(t)$, generated by the stochastic dynamics (7) and $p_{\infty}(x, t) = \lim_{n \rightarrow \infty} p(x, t+nT)$ is the periodic pdf. We obtain in a similar manner

$$P_L(c, \omega, A_{Appl, Ind}, \varepsilon) = \frac{1}{T} \int_0^T \int_{-\infty}^{\tilde{x}_M(t)} p_{\infty}(x, t) dx dt, \quad (11)$$

For small ε ,

$$P_L(c, \omega, A_{Appl, Ind}, \varepsilon) \approx \frac{\bar{\tau}_L}{\bar{\tau}_R + \bar{\tau}_L}. \quad (12)$$

3 The Fokker-Planck equation

The T -periodic pdf $p_{\infty}(x, t)$ is the T -periodic solution of the Fokker-Planck equation

$$\frac{\partial p(x, t)}{\partial t} = \varepsilon \frac{\partial^2 p(x, t)}{\partial x^2} + \frac{\partial[\phi_x(x, t)p(x, t)]}{\partial x} \quad \text{for } -\infty < x < \infty, 0 < t < \infty. \quad (13)$$

We construct a WKB approximation to $p_{\infty}(x, t)$ for small ε ,

$$p_{\infty}(x, t) \sim \frac{\exp\left\{-\frac{\psi(x, t, \varepsilon)}{\varepsilon}\right\}}{\int_{-\infty}^{\infty} \exp\left\{-\frac{\psi(x, t, \varepsilon)}{\varepsilon}\right\} dx}, \quad (14)$$

where $\psi(x, t, \varepsilon)$ is a T -periodic regular function of ε . Expanding

$$\psi(x, t, \varepsilon) = \psi(x, t, 0) + \varepsilon\psi_1(x, t) + \dots, \quad (15)$$

we find from large deviations theory that $\psi(x, t, 0)$ is the minimum of the integral

$$I(x(\cdot))(x, t) = \int_0^t [\dot{x}(s) + \phi_x(x(s), s)]^2 ds \quad (16)$$

over all continuous trajectories $x(\cdot)$ such that $x(0) = x$. Setting $\tau = \omega t$, we write the Hamilton-Jacobi (eikonal) equation for the minimal values of $I(x, \tau)$ in the domains $x > 0$ and $x < 0$ as

$$-\psi_\tau^i(x, \tau, 0) = \frac{1}{\omega} (\psi_x^i)^2(x, \tau, 0) - \frac{1}{\omega} \left[c - A_{Appl, Ind} \sin \tau + \frac{2(x - x_i)}{x_i^2} \right] \psi_x^i(x, \tau, 0), \quad (17)$$

for $i = L, R$. The solution can be constructed in the quadratic form [17]

$$\psi^i(x, \tau, 0) = \frac{[x - \tilde{x}_i(\tau)]^2}{x_i^2} + a_i \quad (18)$$

and the constants a_i are determined from the Freidlin-Wentzell extremum principle [16]. According to this principle the local minima $\psi^L(x, \tau, 0)$ and $\psi^R(x, \tau, 0)$ are joined into a global minimum function $\psi(x, \tau, 0)$ by the requirement that the steady state probability current across the separatrix \tilde{x}_M vanishes [17],

$$J(0, \tau) = \int_0^{2\pi} [J_L(0, \tau) + J_R(0, \tau)] d\tau = 0, \quad (19)$$

where the probability flux density is

$$J_i(0, \tau) = -\varepsilon \frac{\partial p^i(0, \tau)}{\partial x} + \phi_x(0, \tau) p^i(0, \tau) = -\varepsilon \frac{\partial p^i(0, \tau)}{\partial x}. \quad (20)$$

Using the WKB approximation (14) for $p(x, \tau)$, we find that the minimum condition is

$$J_i(0, \tau) = \frac{-2\tilde{x}_i(\tau)}{x_i^2} \exp \left\{ -\frac{1}{\varepsilon} \left(\frac{\tilde{x}_i^2(\tau)}{x_i^2} + a_i \right) \right\}. \quad (21)$$

Using (21) in (19), we find that

$$e^{(a_L - a_R)/\varepsilon} = -\frac{x_R^2 \int_0^{2\pi} \tilde{x}_L(\tau) \exp \left\{ -\frac{\tilde{x}_L^2(\tau)}{\varepsilon x_L^2} \right\} d\tau}{x_L^2 \int_0^{2\pi} \tilde{x}_R(\tau) \exp \left\{ -\frac{\tilde{x}_R^2(\tau)}{\varepsilon x_R^2} \right\} d\tau}. \quad (22)$$

It should be noted that the phases $\tilde{\varphi}_L$ and $\tilde{\varphi}_R$ may be disregarded in the integrals of equation (22), therefore we set them to zero. Expanding the integrals in (22) by the Laplace method for small ε about the maxima of the integrands, at

$$x_1 = \tilde{x}_R(0) = \alpha_R - \tilde{A}_R, \quad x_2 = \tilde{x}_L(\pi) = \alpha_L - \tilde{A}_L, \quad (23)$$

we get

$$\begin{aligned}
e^{(a_L - a_R)/\varepsilon} &= -\frac{x_R^2 \sqrt{\frac{2\pi\varepsilon x_L^2}{[\tilde{x}_L^2]''(\pi)}} \tilde{x}_L(\pi) \exp\left\{-\frac{\tilde{x}_L^2(\pi)}{\varepsilon x_L^2}\right\}}{x_L^2 \sqrt{\frac{2\pi\varepsilon x_R^2}{[\tilde{x}_R^2]''(0)}} \tilde{x}_R(0) \exp\left\{-\frac{\tilde{x}_R^2(0)}{\varepsilon x_R^2}\right\}} \\
&= -\frac{x_R^2 \sqrt{\frac{x_L^2}{-2\tilde{A}_L x_2}} x_2 \exp\left\{-\frac{x_2^2}{\varepsilon x_L^2}\right\}}{x_L^2 \sqrt{\frac{x_R^2}{2\tilde{A}_R x_1}} x_1 \exp\left\{-\frac{x_1^2}{\varepsilon x_R^2}\right\}}, \tag{24}
\end{aligned}$$

where, according to (5) and $\tilde{\varphi}_i = 0$

3.1 The left probability $P_L(c, \omega, A_{Appl, Ind}, \varepsilon)$

To calculate the probability $P_L(c, \omega, A_{Appl, Ind}, \varepsilon)$, we use the WKB approximation (14) in (11) and evaluate the integrals by the Laplace method, as in (21), to get

$$P_L(c, \omega, A_{Appl, Ind}, \varepsilon) = \frac{1}{1 + \frac{x_R}{-x_L} e^{(a_L - a_R)/\varepsilon}}. \tag{25}$$

Using the result from (24) in (25), we find that

$$P_L(c, \omega, A_{Appl, Ind}, \varepsilon) = \frac{1}{1 + \frac{x_R^3}{|x_L|^3} \sqrt{\frac{\sqrt{4 + x_L^4 \omega^2}}{\sqrt{4 + x_R^4 \omega^2}}} \sqrt{\frac{-x_2}{x_1}} \exp\left\{\frac{x_1^2}{\varepsilon x_R^2} - \frac{x_2^2}{\varepsilon x_L^2}\right\}}. \tag{26}$$

We normalize the frequency-dependent left probability $P_L(c, \omega, A_{Appl, Ind}, \varepsilon)$ by the left probability of the unforced dynamics $P_L^0(c, \omega, A_{Appl, Ind} = 0, \varepsilon)$. To calculate $P_L^0(c, \omega, A_{Appl, Ind} = 0, \varepsilon)$, we set $A = 0$ in (25) and obtain

$$P_L^0(c, \omega, A_{Appl, Ind} = 0, \varepsilon) = \left[1 + \frac{x_R^2}{x_L^2} \left| \frac{2 - cx_L}{2 - cx_R} \right| \exp\left\{\frac{c(x_R - x_L)}{\varepsilon} \left(\frac{c(x_R + x_L)}{4} - 1\right)\right\}\right]^{-1}. \tag{27}$$

Note that (27) is not other than (12), where

$$\bar{\tau}_i = \sqrt{\frac{2\pi\varepsilon}{\phi_{xx}^i(\tilde{x}_i) |\phi_x^i(\tilde{x}_M)|^2}} \exp\left(\frac{\phi^i(\tilde{x}_M) - \phi^i(\tilde{x}_i)}{\varepsilon}\right). \tag{28}$$

The MFPT $\bar{\tau}_i$ in (28) is the Kramers escape rate of a Brownian particle over a high sharp barrier \tilde{x}_M [19].

4 Coarse-grained Markov model of secondary gating

We consider the movement of a Brownian particle over two unequal barriers of heights $\Delta\phi_{21} = \phi(x_2) - \phi(x_1)$ and $\Delta\phi_{43} = \phi(x_4) - \phi(x_3)$, respectively, such that $\Delta\phi_{21} \ll \Delta\phi_{43}$ (see Figure 7). Both x_1 and x_3 are closed states of the channel whereas x_5 represents the open state (see Figure 5). Our goal is to elucidate the influence of SR between the periodic force and the activation over the local small barrier $\Delta\phi_{21}$ at x_2 , within the closed state, on the open probability of the channel. Specifically, when SR increases the time spent in the well at x_3 relative to that at x_1 , the attempt frequency to cross the barrier at x_4 into the open state x_5 increases, thus increasing the open probability of the channel. More specifically, we evaluate the influence of SR on the mean closed time, that is, on the mean time spent in the wells at x_1 and x_3 prior to passage into x_5 (which we denote $\bar{\tau}_{1,3}^c$). For that purpose, we can assume that x_5 is an absorbing boundary.

First, we note that steady state considerations can be applied in describing SR in the wells at x_1 and x_3 . Indeed, we assume that

$$\phi(x_4) - \phi(x_5), \phi(x_4) - \phi(x_3) > \phi(x_2) - \phi(x_1) > \phi(x_2) - \phi(x_3) \gg \varepsilon, \quad (29)$$

which means that a transition over the barrier at x_4 between the open and closed states occurs at a much lower rate than those over the barrier at x_2 , between the two closed substates. In particular, the first inequality in (29) means that there will be many transitions over the barrier at x_2 before a transition occurs from x_3 to x_5 over the barrier at x_4 . Thus we confine our attention to transitions over the former and consider x_5 to be an absorbing state, as mentioned above. The assumption of high barriers (the last inequality in (29) means that a quasi steady state is reached in each of the wells before a transition over x_4 occurs. Therefore the pdf of the quasi-steady state in each well can be represented by the principal eigenfunction and eigenvalue in that well, with absorbing boundary conditions.

We coarse-grain the trajectory of the diffusion process $x(t)$ into that of a continuous-time three state Markov jump process $\tilde{x}(t)$, that jumps between x_1 and x_3 and is absorbed in x_5 ,

$$x_1 \rightleftharpoons x_3 \rightarrow x_5. \quad (30)$$

The three state continuous-time Markov chain $\tilde{x}(t)$ is not stationary due to the passage to the open state x_5 . There are two time scales of passages: a short scale corresponding to the transitions between x_1 and x_3 , and a long one for the transitions between x_3 and x_5 . Due to the long time scale, the dynamics between the closed states (x_1 and x_3) is quasi-stationary. We assume it as a stationary dynamics in our analysis.

The jump of the Markov process from x_1 to x_3 occurs when $x(t)$ reaches x_3 for the first time after it was at x_1 , and so on. The Chapman-Kolmogorov equation for the transition probability matrix \mathbf{P}_t of the Markov process is [15]

$$\dot{\mathbf{P}}_t = \mathbf{P}_t \mathbf{R}, \quad (31)$$

where

$$P_t(i, j) = \Pr\{\tilde{x}(t) = j \mid \tilde{x}_0 = i\}, \quad \text{for } 1 \leq i, j \leq 3, \quad (32)$$

and the elements of the instantaneous jump rate matrix \mathbf{R} are

$$\mathbf{R} = \begin{bmatrix} -r_{13} & r_{13} & 0 \\ r_{31} & -(r_{31} + r_{35}) & r_{35} \\ 0 & 0 & 0 \end{bmatrix}. \quad (33)$$

The stationary distribution $\boldsymbol{\pi}$ of the process is

$$\boldsymbol{\pi} = [0, 0, 1],$$

because x_5 is an absorbing state.

Next, we calculate the time-dependent probability distribution

$$\mathbf{p}_t = [\Pr\{\tilde{x}(t) = x_1\}, \Pr\{\tilde{x}(t) = x_3\}, \Pr\{\tilde{x}(t) = x_3\}]^T. \quad (34)$$

According to (31) and (32), \mathbf{p}_t the sum of elements in each column of the matrix \mathbf{P}_t

$$\Pr\{\tilde{x}(t) = x_j\} = \sum_{i=1}^3 \Pr\{\tilde{x}(t) = j \mid \tilde{x}_0 = i\} \quad \text{for } 1 \leq j \leq 3$$

and therefor satisfies the Chapman-Kolmogorov equation

$$\dot{\mathbf{p}}_t = \mathbf{R}^T \mathbf{p}_t, \quad (35)$$

given by

$$\mathbf{p}_t = e^{\mathbf{R}^T t} \mathbf{p}_0, \quad (36)$$

where we assume that \mathbf{p}_0 is the stationary distribution of the chain $x_1 \rightleftharpoons x_3$, namely,

$$\mathbf{p}_0 = \left[\frac{r_{31}}{r_{13} + r_{31}}, \frac{r_{13}}{r_{13} + r_{31}}, 0 \right]^T. \quad (37)$$

We further express the vector \mathbf{p}_t as a linear combination of the eigenvectors $\{\mathbf{v}_1, \mathbf{v}_2, \mathbf{v}_3\}$ of the matrix \mathbf{R}^T , corresponding to the eigenvalues $\lambda_1, \lambda_2, \lambda_3$,

$$\mathbf{p}_t = \alpha_1 e^{\lambda_1 t} \mathbf{v}_1 + \alpha_2 e^{\lambda_2 t} \mathbf{v}_2 + \alpha_3 e^{\lambda_3 t} \mathbf{v}_3, \quad (38)$$

where

$$\lambda_1 = \frac{-r_{13}r_{35}}{S} \quad (39)$$

$$\lambda_2 = -S + \frac{r_{13}r_{35}}{S} \quad (40)$$

$$\lambda_3 = 0. \quad (41)$$

and $S = r_{13} + r_{31} + r_{35}$. Using the fact that $\lim_{t \rightarrow \infty} \mathbf{p}_t = \boldsymbol{\pi}$, we get that $\alpha_3 = 1$.

The MFPTs $\bar{\tau}_3$ and $\bar{\tau}_1$ are related to the exit rates r_{31} and r_{13} over a non-sharp boundary [18] according to

$$\begin{aligned}\bar{\tau}_3 &= \frac{1}{2r_{31}} \\ \bar{\tau}_1 &= \frac{1}{2r_{13}}.\end{aligned}\quad (42)$$

In order to find mean closed time $\bar{\tau}_{1,3}^c$ prior to the first arrival to x_5 , it is enough to consider the matrix

$$\tilde{\mathbf{R}}^T = \begin{bmatrix} -r_{13} & r_{31} \\ r_{13} & -(r_{13} + r_{35}) \end{bmatrix}, \quad (43)$$

because this time is determined by the first two elements of the vector \mathbf{p}_t ,

$$\mathbf{p}_t^{1,3} = \left[\Pr\{\tilde{x}(t) = x_1\}, \Pr\{\tilde{x}(t) = x_3\} \right]^T. \quad (44)$$

An eigenvector expansion $\mathbf{p}_t^{1,3}$, similar to that in (38), is

$$\mathbf{p}_t^{1,3} = \alpha_1 e^{\lambda_1 t} \tilde{\mathbf{v}}_1 + \alpha_2 e^{\lambda_2 t} \tilde{\mathbf{v}}_2, \quad (45)$$

where λ_1 and λ_2 are given in (39) and (40), respectively, and $\tilde{\mathbf{v}}_1$ and $\tilde{\mathbf{v}}_2$ are the eigenvectors of the matrix $\tilde{\mathbf{R}}^T$

$$\begin{aligned}\tilde{\mathbf{v}}_1 &= [r_{31}S, r_{13}S - r_{13}r_{35}]^T \\ \tilde{\mathbf{v}}_2 &= [r_{31}S, r_{13}S - S^2 + r_{13}r_{35}]^T.\end{aligned}$$

Using the initial condition

$$\mathbf{p}_0^{1,3} = \left[\frac{r_{31}}{r_{13} + r_{31}}, \frac{r_{13}}{r_{13} + r_{31}} \right]^T,$$

we obtain

$$\alpha_1 = \frac{S^2 + r_{13}r_{35}}{S^3(r_{13} + r_{35})} \approx \frac{1}{(r_{13} + r_{31})^2}, \quad \alpha_2 = \frac{r_{13}r_{35}}{-S^3(r_{13} + r_{31})}.$$

Setting $P(t) = \mathbf{p}_t^{1,3}(1, 1) + \mathbf{p}_t^{1,3}(2, 1)$ and substituting the values of α_1 , α_2 , $\tilde{\mathbf{v}}_1$ and $\tilde{\mathbf{v}}_2$ into (45), we obtain

$$P(t) = e^{\lambda_1 t} - e^{\lambda_2 t} \frac{(r_{13}r_{35})^2}{(r_{13} + r_{31})^4}. \quad (46)$$

Hence

$$\bar{\tau}_{1,3}^c = E[\tau_{1,3}^c] = \int_0^\infty P(t) dt \sim \frac{1}{|\lambda_1|} = \frac{S}{r_{13}r_{35}} \simeq \frac{1}{r_{35}} \left(1 + \frac{r_{31}}{r_{13}} \right). \quad (47)$$

Using (42) in (47) and setting $P_3^R = \frac{\bar{\tau}_3}{\bar{\tau}_3 + \bar{\tau}_1}$, we obtain that

$$\bar{\tau}_{1,3}^c = \frac{1}{r_{35}} \left(1 + \frac{\bar{\tau}_1}{\bar{\tau}_3} \right) = \frac{1}{r_{35}} \frac{1}{P_3^R}, \quad (48)$$

We further coarse-grain the trajectories of the process $\tilde{x}(t)$ into that of a telegraph process with two states, closed state (corresponding to x_1 and x_3) and open state (corresponding to x_5)

$$c \rightarrow o.$$

Denoting $\bar{\tau}_o$ as the mean first passage time from x_5 , using equation (48) we get

$$P_{open} = \frac{\bar{\tau}_o}{\bar{\tau}_o + \bar{\tau}_{1,3}^c} = \frac{\bar{\tau}_o}{\bar{\tau}_o + \frac{1}{r_{35}} \frac{1}{P_3^R}}. \quad (49)$$

Applying the theory proposed in 3.1, to the dynamics between the closed states x_1 and x_3 , the SR effect increases P_3^R , by using a negative depolarization, c . According to (49) an increase of P_3^R causes to an increase of P_{open} .

4.1 High barrier approximation to r_{35} , r_{31} , r_{13}

We consider the autonomous stochastic differential equation

$$dx = -\phi'(x) dt + \sqrt{2\varepsilon} dw \quad (50)$$

$$x(0) = x.$$

The transition rates between the wells are the probability fluxes in the direction of the transition at the top of the barrier. Thus, denoting by $\Phi_i(x)$ and λ_i the principal eigenfunction and eigenvalue in well i ($i = 1, 3$), we have

$$r_{13} = -\varepsilon \Phi_1'(x_2), \quad r_{31} = \varepsilon \Phi_3'(x_2), \quad r_{35} = -\varepsilon \Phi_3'(x_4). \quad (51)$$

To calculate the fluxes, we have to construct the eigenfunctions $\Phi_i(x)$, which are the solutions of

$$\varepsilon \Phi_1''(x) + [\phi'(x)\Phi_1(x)]' = -\lambda_1 \Phi_1(x) \quad \text{for } -\infty < x < x_2 \quad (52)$$

$$\Phi_1(x_2) = 0, \quad \Phi_1(x) \rightarrow 0 \quad \text{for } x \rightarrow -\infty \quad (53)$$

$$\varepsilon \Phi_3''(x) + [\phi'(x)\Phi_3(x)]' = -\lambda_3 \Phi_3(x) \quad \text{for } -x_2 < x < x_4 \quad (54)$$

$$\Phi_3(x_2) = 0, \quad \Phi_3(x_4) = 0. \quad (55)$$

The asymptotic structure of the eigenfunctions is given in [19] as

$$\Phi_1(x) \sim -\mathcal{N}_1^{-1} e^{-\phi(x)/\varepsilon} \sqrt{\frac{2}{\pi}} \int_0^{\omega_2(x-x_2)/\sqrt{\varepsilon}} e^{-z^2/2} dz \quad \text{for } x < x_2 \quad (56)$$

$$\Phi_3(x) \sim \mathcal{N}_3^{-1} e^{-\phi(x)/\varepsilon} \sqrt{\frac{2}{\pi}} \left[\int_{\omega_4(x-x_3)/\sqrt{\varepsilon}}^{\omega_2(x-x_2)/\sqrt{\varepsilon}} e^{-z^2/2} dz - 1 \right] \quad \text{for } x_2 < x < x_4, \quad (57)$$

where $\omega_i = \sqrt{|\phi''(x_i)|}$, ($i = 1, 2, 3, 4$) and

$$\mathcal{N}_1 = \int_{-\infty}^{x_2} \Phi_1(x) dx \sim \frac{\sqrt{2\pi}}{\omega_1} e^{-\phi(x_1)/\varepsilon}, \quad \mathcal{N}_3 = \int_{x_2}^{x_4} \Phi_3(x) dx \sim \frac{\sqrt{2\pi}}{\omega_3} e^{-\phi(x_3)/\varepsilon}. \quad (58)$$

According to (51) and (56)-(58),

$$r_{13} \sim \frac{\omega_1 \omega_2}{\pi} e^{-[\phi(x_2) - \phi(x_1)]/\varepsilon}, \quad r_{31} \sim \frac{\omega_3 \omega_2}{\pi} e^{-[\phi(x_2) - \phi(x_3)]/\varepsilon}, \quad r_{35} \sim \frac{\omega_3 \omega_4}{\pi} e^{-[\phi(x_4) - \phi(x_3)]/\varepsilon}, \quad (59)$$

which are Kramers' rates for the corresponding barriers [19].

5 Effect of SR in the Luo-Rudy model of cardiac myocytes

The Luo-Rudy model [3] describes ionic concentrations and cardiac ventricular action potential by a system of 21 ordinary differential equations. It reflects the guinea-pig electrophysiology by detailed Hodgkin-Huxley models of ionic currents. The most significant currents are the slow I_{Ks} and rapid I_{Kr} delayed rectifier potassium currents, a time-independent potassium current, a plateau potassium current (ultra-rapid I_{Kur}), a transient outward current, fast and background sodium currents, L- and T-type calcium currents, a background calcium current, calcium pumps, sodium-potassium pumps, and sodium-calcium exchangers. In addition, the model describes Ca^{2+} handling processes, that is, calcium dynamic release from the sarcoplasmic-reticulum and from the calcium buffers troponin, calmodulin, and calsequestrin.

The stochastic resonance described above changes the open probability of the I_{Ks} channel, and therefore it affects its conductance. To incorporate this effect into the Luo-Rudy model, we modify the Hodgkin-Huxley equation for the I_{Ks} current-voltage relation by shifting the stationary open probability of the channel in the Luo-Rudy model [3],

$$P_O(V) = \frac{1}{1 + \exp \left\{ -\frac{V - 1.5}{16.7} \right\}}, \quad (60)$$

to

$$\tilde{P}_O(V) = \frac{1}{1 + \exp \left\{ -\frac{V + 4.12}{16.7} \right\}}, \quad (61)$$

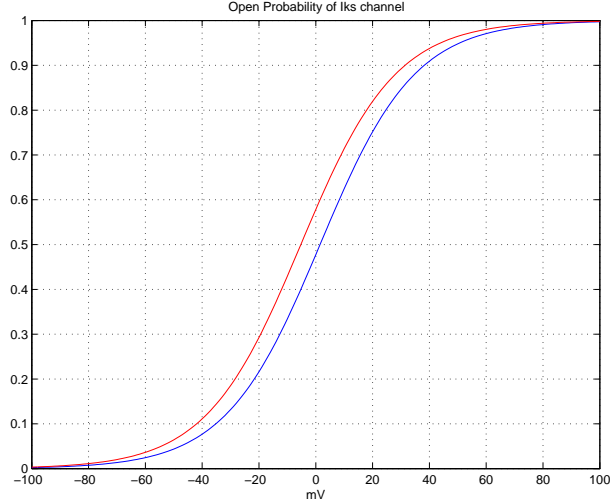


Figure 17: Resonant increase (red) of 20% in the open probability of the I_{Ks} channel, and normal regime (blue)

which imitates the experimentally observed shift (see figure 1). This changes the channel conductance $\bar{G}_{Ks}P_O^2(V)$ in the Luo-Rudy model (\bar{G}_{Ks} is the open channel conductance) to $\bar{G}_{Ks}\tilde{P}_O^2(V)$, which changes, in turn, the membrane potassium current $\langle I_{Ks} \rangle$, averaged over many channels, to [3]

$$\langle I_{Ks} \rangle \rightarrow \bar{G}_{Ks}\tilde{P}_O^2(V)(V - E_{Ks}) \quad \text{as } t \rightarrow \infty \quad (62)$$

(E_{Ks} is the reversal potential of the channel). The effect of this modification of the Luo-Rudy model is shown in Figure 11. The duration of the action potential is reduced and accordingly, the peak of the cytosolic calcium concentration is lowered (see Figures 12), as in the experiment described in the Introduction. On the other hand, sodium concentration is increased (see Figure 13). The shortening of the action potential duration in the ventricular cardiac myocytes affects the QT interval in the electrocardiogram, which consists of a sum of several different action potentials created in the myocardium [10] (see Figures 14, 15). These theoretical predictions are supported by experimental measurements. Specifically, these effects in vivo were communicated in [13], [14], as well as in our own in vitro measurements [2].

6 Conclusion and Discussion

This paper tries to explain the results of the experiment of exposing human potassium I_{Ks} channels and cardiac myocytes, which contain these channels, to weak and slow electromagnetic fields. We offer a scenario of a new kind of stochastic resonance between the induced periodic field and the thermally activated transitions between locally stable configurations of the mobile ions in the selectivity filter.

More specifically, since the induced electric field is too weak to interact with any component of the I_{Ks} channel protein, our model cannot describe the primary gating mechanism

of a voltage gated channel. We therefore resort to a mathematical model, which postulates interaction of the induced field with configurations of the mobile ions inside the selectivity filter. These configurations may be much more susceptible to the weak induced field than any components of the surrounding protein, because the potential barriers separating the metastable configurations of the mobile ions can be of any height.

According to our scenario, the observed resonance is due to the dependence of the induced electric field amplitude on frequency, in contrast to an applied external electric field with fixed frequency, which is known not to exhibit stochastic resonance with changing frequency and depolarization. In our theory the observed SR between two closed (or inactivated) states affects the open probability of the channel.

Our model describes the dynamics of a Brownian particle in an *asymmetric* bistable potential forced by a periodic *induced* electric field. The analysis of this model is based on the construction of an asymptotic solution to the time-periodic Fokker-Planck equation in the WKB form. We evaluate the dependence of the steady state probability to be on one side of the potential barrier on the frequency, amplitude, depolarization, and noise intensity.

Our main results are shown in Figure 10, which indicates that there is a peak in the open probability in a relatively narrow range of depolarizations and frequencies. We refer to this peak as stochastic resonance, though it is not be the usual SR phenomenon. This observation is consistent with the results of the I_{Ks} channel experiment mentioned in the Introduction.

Another result is the incorporation of the SR result into the Luo-Rudy model of cardiac myocytes. We found that the increased conductance of the I_{Ks} channel reduces the duration of the action potential, the peak height of the cytosolic calcium concentration, in good agreement with the experimental results. The shortening of the action potential duration in the ventricular cardiac myocytes affects the QT interval in the electrocardiogram.

Acknowledgment: We wish to thank S. Laniado, T. Kamil and M. Scheinowitz for introducing us to the *in vivo* resonance experiments, T. Zinman, A. Shainberg and S. Barzilai for the *in vitro* cardiac myocytes experiments, G. Gibor and B. Attali for the oocyte experiments, and N. Dascal and A. Moran for experiments on L-type channels. We thank Y. Rudy, F. Bezanilla, and G. Deutscher for useful discussions.

References

- [1] M. Shaked, G. Gibor, B. Attali and Z. Schuss, "Weak EMF at 16 Hz increases conductance of I_{Ks} and KCNQ1 channels in a narrow window of depolarizations", (preprint 2009).
- [2] M. Shaked, T. Zinman, A. Shainberg and Z. Schuss, "The effect of extremely low frequency and amplitude electromagnetic fields in cytosolic calcium of cardiac myocytes", (preprint 2009).

- [3] J. Zeng, K.R. Laurita, D.S. Rosenbaum, Y. Rudy, "Two components of the delayed rectifier K^+ current in ventricular myocytes of the Guinea pig type", *Circ. Res.* **77**, pp.140–152 (1995).
- [4] S. Bernèche and B. Roux, "Energetics of ion conduction through the K^+ channel", *Nature*, **414**, pp.73-77 (2001).
- [5] L. Gammaitoni, P. Hänggi, P. Jung, and F. Marchesoni, "Stochastic Resonance", *Rev. Mod. Phys.* **70**, pp.223–288 (1998).
- [6] A. Nikitin, N. G. Stocks and A. R. Bulsara, "Asymmetric bistable systems subject to periodic and stochastic forcing in the strongly nonlinear regime: Switching time distributions", *Phys. Rev E* **68**, 016103 (2003).
- [7] H.S. Wio and S. Bouzat, "Stochastic Resonance: The role of Potential Asymmetry and Non Gaussian Noises", *Brazilian Journal of Physics* **29** (1), pp.1-8 (1999).
- [8] J.H. Li, "Effect of asymmetry on stochastic resonance and stochastic resonance induced by multiplicative noise and by mean-field coupling", *Phys. Rev. E* **66**, pp.0311041-0311047 (2002).
- [9] A. L. Hodgkin and A. F. Huxley, "A Quantitative Description of Membrane Current and its Application to Conduction and Excitation in Nerve", *J. Physiology* **117**, pp.500–544 (1952).
- [10] L.H. Opie, *Heart Physiology: From Cell to Circulation*, Lippincott, Williams & Wilkins; 4th edition 2003.
- [11] C. Koch, *Biophysics of Computation*, Oxford University Press, NY 1999.
- [12] D. Johnston and S.M. Wu, *Foundations of Cellular Neurophysiology*, MIT Press, Cambridge, MA 1995.
- [13] R. Mazhari, H.B. Nuss, A.A. Armourdas, R.L. Winslow, E. Marban, "Ectopic expression of KCNE3 accelerates cardiac repolarization and abbreviates the QT interval", *J. Clin. Invest.* **109**, pp.1083-1090 (2002).
- [14] J.H. Jeong, J.S. Kim, B.C. Lee, Y.S. Min, D.S. Kim, J.S. Ryu, K.S. Soh, K.M. Seo, U.D. Sohn, "Influence of exposure to electromagnetic field on the cardiovascular system", *Autonomic & Autacoid Pharmacology* **25** (1), pp.17-23 (7) (2005).
- [15] S.M. Ross, *Stochastic Processes*, John Wiley & Sons, Inc. NY 1983.
- [16] M.A. Freidlin and A.D. Wentzell, *Random Perturbations of Dynamical Systems*, Springer-Verlag, NY 1984.
- [17] R. Graham and T. Tél, "Weak-noise limit of Fokker-Planck models and nondifferentiable potentials for dissipative dynamical systems", *Phys.Rev A* **31** (2), pp.1109–1122 (1985).

- [18] B.J. Matkowsky, Z. Schuss and C. Tier “Uniform expansion of the transition rate in Kramers’ problem”, *J. Stat. Phys.* **35**(3/4), pp. 443–456 (1984).
- [19] Z. Schuss, *Theory and Applications of Stochastic Differential Equations*, Wiley, NY 1980.